Original Article

GMSMJ

Greater Mekong Subregion Medical Journal

Exploring Potential of Phytochemicals from Houttuynia cordata Thunb. as Angiogenesis Inhibitors in Melanoma Treatment: A Molecular Docking Study

Mongkol Yanarojana, M.D.[1], Thamthiwat Nararatwanchai, M.D. Ph.D.[1], Salunya Tancharoen, D.D.S., Ph.D.[2], Somchai Yanarojana, M.D., Ph.D.[3]

[1]School of Anti-Aging and Regenerative Medicine, Mae Fah Luang University, Bangkok, Thailand 10110

[2]Department of Pharmacology, Faculty of Dentistry, Mahidol University, Bangkok, Thailand 10400

[3]Department of Pharmacology, Faculty of Science, Mahidol University, Bangkok, Thailand 10400

Received 6 February 2025 • Revised 11 August 2025 • Accepted 3 September 2025 • Published online 1 January 2026

Abstract:

Background: *Houttuynia cordata* Thunb. extract has shown programmed cell death induction in melanoma. Antagonism of the VEGF receptors (VEGFR) has been suggested as a potential mechanism of action due to its role in the progression of melanoma. Given the downsides of the current anti-VEGFR drugs, including lack of selectivity and unwanted side effects, the phytochemical constituents of *Houttuynia cordata* Thunb. were investigated for their inhibition of VEGFR using molecular docking simulations.

Objective: To investigate and identify the efficacy of potential orally-compatible phytochemical constituents that bind and inhibit the ATP binding sites of VEGFR1 and VEGFR2 using molecular docking simulations.

Materials and Method: The X-ray crystal structures of VEGFR1 and VEGFR2 were downloaded and prepared. A total of 74 phytochemical compounds in *Houttuynia cordata* Thunb. were constructed and energy minimized in 3D format and docked to the ATP binding sites of VEGFR1 and VEGFR2. Drug-like properties were calculated. This is followed by analysis of the binding modes, calculated docking scores and oral pharmacokinetics of potential candidates.

Results: Five compounds, luteolin, quercetin, isorhamnetin, apigenin, and kaempferol, were identified to have acceptable oral pharmacokinetics and docking scores, and were predicted *in silico* to have adequate VEGFR inhibition. Notably, apigenin and quercetin were predicted to have the best inhibitory action against VEGFR1 and VEGFR2, respectively, i.e., apigenin scored -9.148 kcal/mol against VEGFR1, and quercetin scored -9.945 kcal/mol against VEGFR2.

Corresponding author: Salunya Tancharoen, D.D.S., Ph.D.
Department of Pharmacology, Faculty of Dentistry, Mahidol University, Bangkok, Thailand 10400
E-mail: salunya.tan@mahidol.ac.th

GMSMJ 2026; 6 (1): 1-10

@2026 GMSMJ. Hosting by Mae Fah Luang University. All rights reserved

Conclusion: Luteolin, quercetin, isorhamnetin, apigenin, and kaempferol could serve as potential candidates for effective inhibition of the ATP binding site of VEGFR. In this light, these phytochemical constituents of *Houttuynia cordata* Thunb. are suggested as potential therapeutics for the treatment of melanoma through direct inhibition of VEGFR at the ATP binding site. Specifically, apigenin and quercetin were predicted to be the strongest VEGFR1 and VEGFR2 inhibitors and are suggested for in *vitro* and in *vivo* drug tests.

Keywords: Melanoma, *Houttuynia cordata*, Quercetin, Apigenin, VEGFR, Angiogenesis, Molecular docking

Introduction

Melanoma, a highly malignant form of skin cancer, is characterized by its aggressive nature and propensity for metastasis, rendering it resistant to conventional therapeutic modalities. In melanoma, angiogenesis is indispensable for the growth and progression of the tumor. Traditionally, angiogenesis is thought to be driven by hypoxia, which occurs when the tumor outgrows its blood supply, leading to low oxygen levels within the cancer.[1] However, recent studies have shown that angiogenesis can occur independently of hypoxia, driven by various signaling pathways such as BRAF V600E, PI3 kinase, ET-1, reactive oxygen species (ROS), NF-κB, MITF, NRAS (with GAB2), ILK, and NRF2.[2] These findings highlight the complex and multifaceted nature of angiogenesis in melanoma, underscoring the need for targeted therapies that can effectively inhibit this process.

Targeted therapies that inhibit angiogenesis, such as the anti-VEGF antibody bevacizumab, have shown promise in clinical trials. Furthermore, combining antiangiogenic therapies with immune checkpoint inhibitors has improved survival outcomes in patients with metastatic melanoma, suggesting a potential synergistic effect. Over the years, the development of angiogenesis inhibitors has become a focal point in the fight against cancer, including melanoma.[3-5]

Houttuynia cordata, commonly known as the Chameleon plant, is a perennial herb for use as a regimen in traditional medicine across Asia. It is renowned for its diverse therapeutic properties which include anti-inflammatory, antimicrobial, antioxidant, promotion of immunity and anticancer activities.[6] Modulation of various molecular pathways by the phytochemical constituents were reported mainly for abundant phytochemical groups which include flavonoids, phenolic acids and polysaccharides. Specifically, polysaccharides have shown promotion of macrophage function and quenching of superoxide radicals, and cytotoxic activities and induction of apoptosis were reported for flavonoids against various cancer cell lines.[6] Given the presence of these phytochemical groups in many dietary supplements, there is a notion that the chemical scaffolds of these phytochemical constituents are viable options to be used for anticancer drug development in the future. This can replace the more cytotoxic drugs that are currently in clinical use, which contain stronger and often, unbearable side effects. However, the role of these phytochemicals as angiogenic inhibitors, particularly for the treatment of melanoma remained largely unexplored.

In treating melanoma, the Vascular Endothelial Growth Factor (VEGF) and its pathway are pivotal targets for inhibiting angiogenesis.[7] VEGF, a primary stimulator

of angiogenesis, plays a critical role in developing new blood vessels within tumors. It is chiefly produced by cancer cells and is instrumental in mediating vascular permeability and facilitating tube formation. In particular, the VEGF receptors (VEGFR) which has a tyrosine kinase domain has been a successful anti-angiogenic drug target for treatment of various cancers.[8] Targeting VEGF pathways has been clinically effective at suppressing melanoma growth and progression, especially in metastatic cases.

Our previous *in vitro* study demonstrated that *Houttuynia cordata* Thunb. extract induces programmed cell death in melanoma by activating the caspase-dependent pathway and p38 phosphorylation associated with HMGB1 reduction.[9] In this study, we conducted a virtual screen by employing molecular docking simulations to study and analyze the interactions between 74 phytochemical constituents from *Houttuynia cordata* Thunb. and the ATP binding site of VEGFR; the ATP binding site has been a target site for mainly phytochemicals and small molecule drugs. This approach allows prediction of the binding affinities and mode of interactions between the phytochemicals and VEGFR, providing insights into their potential efficacies as angiogenesis inhibitors for melanoma therapy. Through this *in silico* analysis, we aim to identify promising orally compatible candidates for development of new therapeutic agents against melanoma.

Materials and method

Retrieval and preparation of ligands for molecular docking

A comprehensive list of 74 phytochemical compounds in *Houttuynia cordata* Thunb. were obtained from Kumar *et al*.,[10] as shown in Table S1 (supplementary materials); the volatile oils were excluded from the selection as these are large structures, which plausibly do not interact with the ATP binding site, and oils in general have been reported to show no direct or weak kinase inhibition, rather a binding site specified for lipids.[11] The structures of seventy-four phytochemical compounds were downloaded from the PubChem database (https://pubchem.ncbi.nlm.nih.gov/)[12, 13] in SDF file format. Furthermore, three drugs sorafenib (CID: 216239), axitinib (CID: 6450551) and pazopanib (CID: 10113978) were downloaded from the same database. The ligand molecules were then prepared using the Open Babel tool (v 2.4.1)[14] of PyRx software (v1.1)[15] by minimizing their energies and following conversion into a PDBQT file format for use in the molecular docking study.

Retrieval and preparation of target proteins for molecular docking

The 3D protein structures were obtained from the RCSB Protein Data Bank (RCSB PDB)[16] in 3D SDF file format: VEGFR1 kinase domain (PDB ID: 3HNG) and VEGFR2 kinase domain (PDB ID: 2XIR). The target receptors were first prepared by removing the solvent molecules and co-crystallized ligands, addition of hydrogen atoms, partial charge adjustments, 3D protonation, and energy minimization using Discovery Studio Visualizer (version 21.1.0.20290).

Molecular Docking Study.

The PyRx with Vina Wizard was utilized in molecular docking experiments to determine the docking scores, ligand binding modes and ligand-protein interactions. The Vina Wizard is a user-friendly interface for running molecular docking simulations with Autodock Vina[17] version 1.2.5 as the molecular docking engine. The prepared structures of target proteins were imported into PyRx and converted into PDBQT file format. An

exhaustiveness value of 20 for the experiment was selected and the best docked conformations were characterized by the lowest docking scores. The Discovery Studio Visualizer was used to visualize the interactions and binding modes between the ligands and receptor proteins.

Results and discussion

The protocol was first verified by removing and re-docking the co-crystallized ligands (compounds 78 and 79) to the VEGFRs at different exhaustiveness values (Table S2 in the supplementary materials). The RMSD values were low for the two co-crystallized ligands at exhaustiveness values at 10, 15 and 20 indicating reproducibility.

Antagonistic potential of the phytochemical constituents in *Houttuynia cordata* Thunb. as VEGFR inhibitors were investigated using molecular docking simulations. The docking scores represent the predicted binding affinities of the compounds are as shown in Table S3 (supplementary materials) and the histogram in Figure 1. The scores range from -4.857 to -10.620 kcal/mol for VEGFR1, and -4.669 to -10.051 kcal/mol for VEGFR2. Hesperidin (compound 14) was predicted to be the strongest inhibitor, whereas 5-methoxy-1-methylpyrrolidin-2-one (compound 61) was the predicted to be the weakest. The docking scores of hesperidin to VEGFR1 are -10.620 kcal/mol, and -10.051 kcal/mol for VEGFR2. However, the structure of the compound is large and is likely orally incompatible. The physicochemical properties of hesperidin (Table 1) were calculated using the DruLiTo web server (http://pitools.niper.ac.in/DruLiToWeb/ DruLiTo_index.html) that showed it to be incompatible for oral drug administration since hesperidin do not adhere to the Lipinski's Rule of Five.[18] Following this, the docking scores of the clinically approved VEGFR inhibitors were evaluated, which include sorafenib, axitinib, and pazopanib. Against VEGFR1, sorafenib, axitinib, and pazopatinib exhibited docking scores of -11.650, -10.498 and -10.398 kcal/mol, respectively. Whereas against VEGFR2, sorafenib, axitinib and pazopatinib exhibited scores of -10.492, -11.267 and -10.496 kcal/mol, respectively. It is apparent that the docking scores of the phytochemical constituents are lower than the clinically approved drugs. This is reasonable as the drugs have a larger van der Waal's surface, *i.e.*, greater hydrophobic and van der Waal's contacts with the surrounding amino acid residues. Secondly, the drugs have been optimized for their pharmacological and clinical effectiveness through multiple stages of development. A threshold value of -9 kcal/mol was used as the cut-off to identify 11 potentially active compounds (Table 1), *i.e.*, 11 compounds with scores of less than -9 kcal/mol were selected as orally compatible VEGFR inhibitor candidates. Amongst the 11 compounds, only 5 adhered to the Lipinski's Rule of Five and were predicted to have acceptable oral bioavailability: luteolin, quercetin, isorhamnetin, apigenin, and kaempferol. From these 5 compounds, apigenin was predicted to have the strongest inhibition against VEGFR1 (-9.148 kcal/mol), and quercetin as the strongest inhibitor against VEGFR2 (-9.945 kcal/mol).

Literature reports have implicated apigenin as an anticancer agent and a suppressor of angiogenesis in human lung cancers by reducing HIF-1α expression, and decrease in endothelial and pericyte motility,[19, 20] in which our findings suggest a new anti-angiogenic mechanism for apigenin, *i.e.*, direct inhibition of the VEGFR kinase domain. On the other hand, quercetin has been reported to reduce VEGFR2 expression in hepatocellular carcinoma,[21] and colorectal cancer[22], decrease migration of VEGF-induced primate choroid-retinal endothelial cells,[23] and suppression of

VEGF induced phosphorylation of VEGFR2 and their downstream protein kinases AKT, mTOR, and ribosomal protein S6 kinase in human umbilical vein endothelial cells.[24] As mentioned, the anti-angiogenic properties of apigenin and quercetin are clearly established. Regardless, none reported direct inhibition of the ATP binding site of VEGFR at the kinase domain, which suggest that our findings are new, and suggest that apigenin and quercetin can potentially inhibit VEGFRs directly contributing to their anti-angiogenic properties. The docking conformations of quercetin and apigenin will be further analyzed for their interactions with the kinase domain of VEGFR, and compared to reference drugs, sorafenib, axitinib, pazopanib, and the re-docked co-crystallized ligands present in VEGFR crystal structures (Figures 2 and 3).

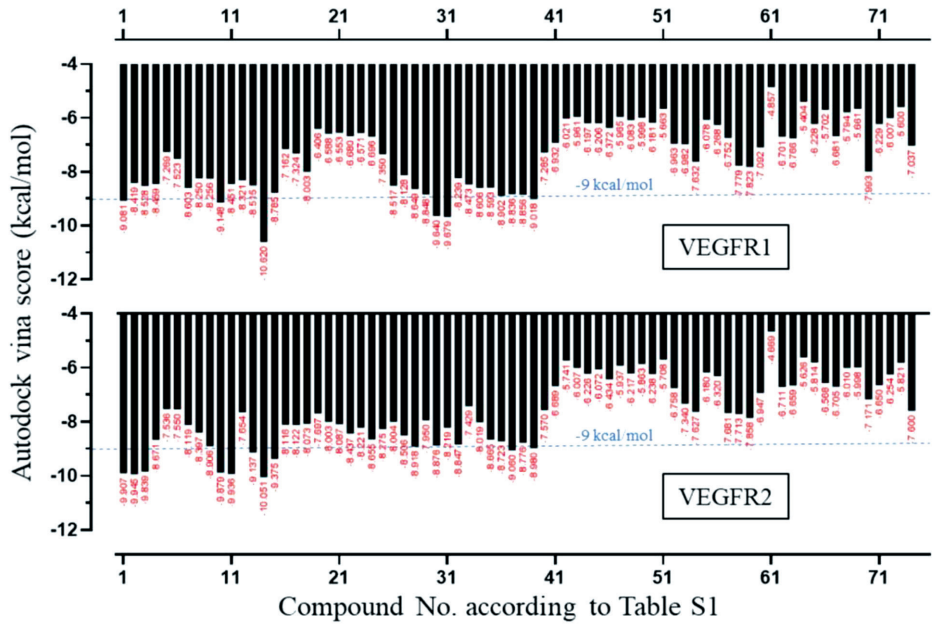

Figure 1 The docking scores calculated using Autodock Vina for the 74 phytochemical compounds from *Houttuynia cordata* Thunb., targeting VEGFR1 and VEGFR2.

Table 1 The docking scores of eleven best scoring candidates and the calculated physicochemical properties.

No.	Name	Docking score (kcal/mol)		Lipinski's rule of five			
		VEGFR1	VEGFR2	MW	Log P	HBD	HBA
1	**Luteolin**	-9.081	-9.907	286.25	1.486	4	6
2	**Quercetin**	-8.419	-9.945	302.24	1.834	5	7
3	**Isorhamnetin**	-8.528	-9.839	316.26	1.726	4	7
10	**Apigenin**	-9.148	-9.879	270.24	1.138	3	5
11	**Kaempferol**	-8.451	-9.936	286.24	1.486	4	6
14	**Hesperidin**	-10.620	-10.051	610.62	-1.110	8	15

The predicted binding mode of apigenin with the ATP binding site of VEGFR1 was analyzed (Figure 2A). It was found that the phenol group was able to form hydrogen bonds with a Cys912, the ketone with Lys861, and a hydroxyl group on the bicyclic ring to residue Glu878. In comparison the docking simulations of the known inhibitors, sorafenib (Figure 2B) and axitinib (Figure 2C) exhibited hydrogen bond formations with Glu878 and Cys912, whereas pazopanib (Figure 2D) and compound 78 (Figure 2E) displayed hydrogen bonds with Glu878. It was established that a pharmacophoric feature of inhibitors of VEGFR1 at the ATP binding site is hydrogen bond formations with residues Cys912 and Glu878, which was seen for the reported inhibitors in the literature.[25-27] These key interactions are important contributions for explaining its prominent docking scores compared to the other compounds. Additionally, hydrophobic interactions were seen for sigma interactions with the π-delocalized system were observed with residues Leu833, Val892, Val909 and Leu1029, whereas alkyl-π interactions were formed with residues Val841, Ala859 and Cys1039. These residues were seen to form π-interactions with the reference drugs used and compound 78. In Figure 2A, it can be seen that the phenol ring of apigenin was inserted into the deep hydrophobic gorge of the ATP binding site, which is consistent with the binding modes of sorafenib, axitinib, pazopanib and compound 78, as the gorge is specific for occupation of hydrophobic aromatic rings. Here, hydrophobic interactions with leucine clusters were observed. Apigenin is mainly hydrophobic and thus, its binding affinity to VEGFR1 can be partly accounted for its non-polar van der Waal's interactions, which were formed with mainly hydrophobic residues: Gly915, Phe1041, Leu882, Val907, Val860 and Tyr911. Additionally, the side chains of residues charged polar residues including Asp1040 and Glu910 were also seen to form the van der Waal's interactions. Residues Asp1040 and Phe1041 are part of the DFG motif, which regulates structural conformational change of VEGFR1, *i.e.*, interactions with these two residues are known to hamper VEGFR1 activity.

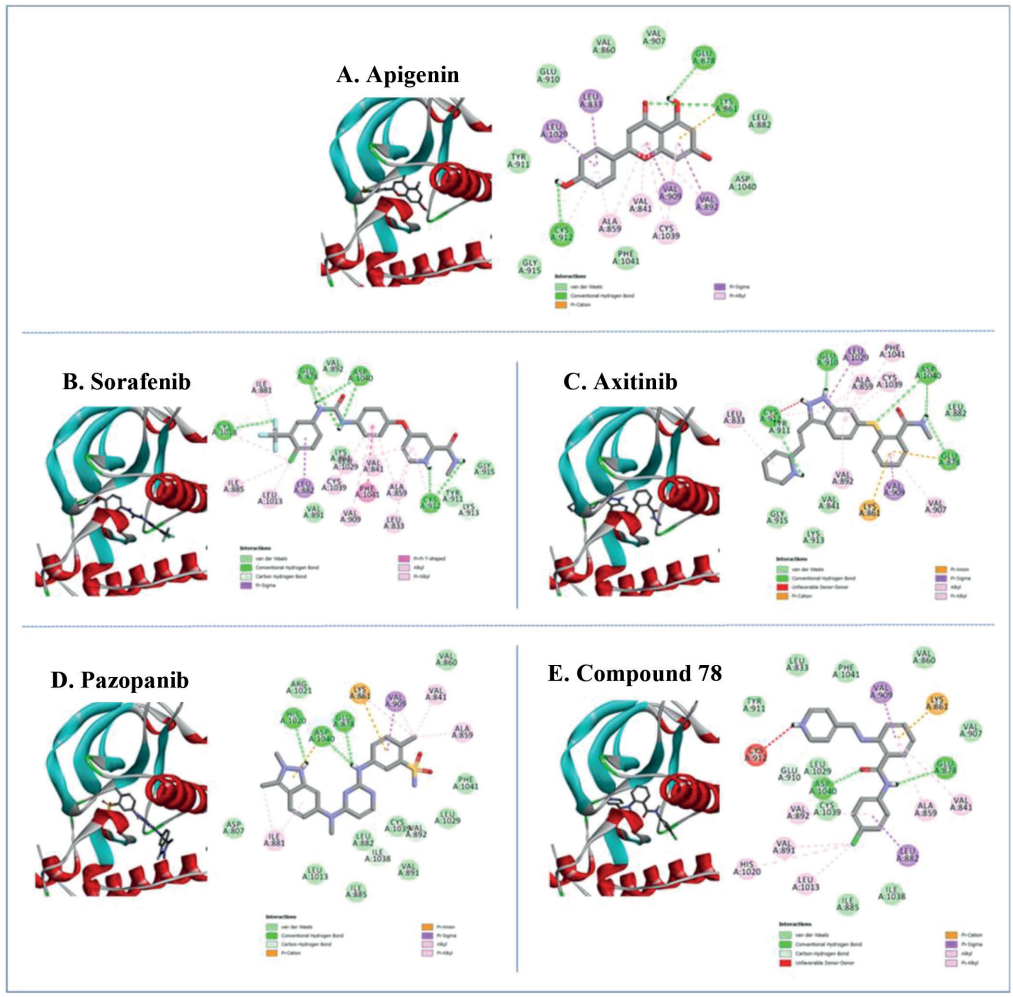

Figure 2 Docked conformations of (A) apigenin, (B) sorafenib, (C) axitinib, (D) pazopanib, and (E) compound 78 (*N*-(4-Chlorophenyl)-2-((pyridin-4-ylmethyl)amino) benzamide) (PDB ID: 3HNG) to the VEGFR1 kinase domain, accompanied by their 2D interaction diagrams.

The predicted binding mode of quercetin with the ATP binding site of VEGFR2 was analyzed (Figure 3A). The structure of the VEGFR2 subtype is very similar and closely related to the VEGFR1 subtype. Hydrogen bonds were formed between quercetin and key pharmacophoric residues Cys919, Asp1046 and Glu917, *i.e.*, interactions with these residues were reported in literature to be important for VEGFR2 inhibition.[28-30] Residue Asp1046 is part of the VEGFR2 DFG motif. Thus, by forming a hydrogen bond interaction with Asp1046, quercetin is able to disrupt the activation mechanism of the receptor. Comparing to the docked conformations of the reference controls, axitinib and compound 79, clearly formed these interactions. Quercetin showed hydrophobic π-interactions; π-sigma between the bicyclic aromatic ring with residues Leu1035 and Leu840, and π-alkyl interactions between phenol ring and residues Ala866, Cys1045, Val916 and Val848. In comparison to the interactions with the reference controls, these amino acid residues were seen to form π-interactions with the controls. The bicyclic ring of quercetin was seen to insert into the hydrophobic gorge of the binding site where hydrophobic interactions and van der Waal's attractions were predicted. Quercetin is mainly hydrophobic. Thus, the binding strength of quercetin to VEGFR2

is accountable for its non -polar and hydrophobic interactions. Non-polar van der Waal's forces were observed between quercetin and mainly hydrophobic residues including Val867, Val899, Phe918, Gly922, Asn923 and Phe1047; Phe1047 is part of the DFG motif in VEGFR2, which recognizes this as a crucial interaction for VEGFR2 inhibition.[29] Other polar residues that contribute to van der Waal's attractions to quercetin include Lys920, Cys1045 and Lys868. These non-polar attractions were observed in the reference controls.

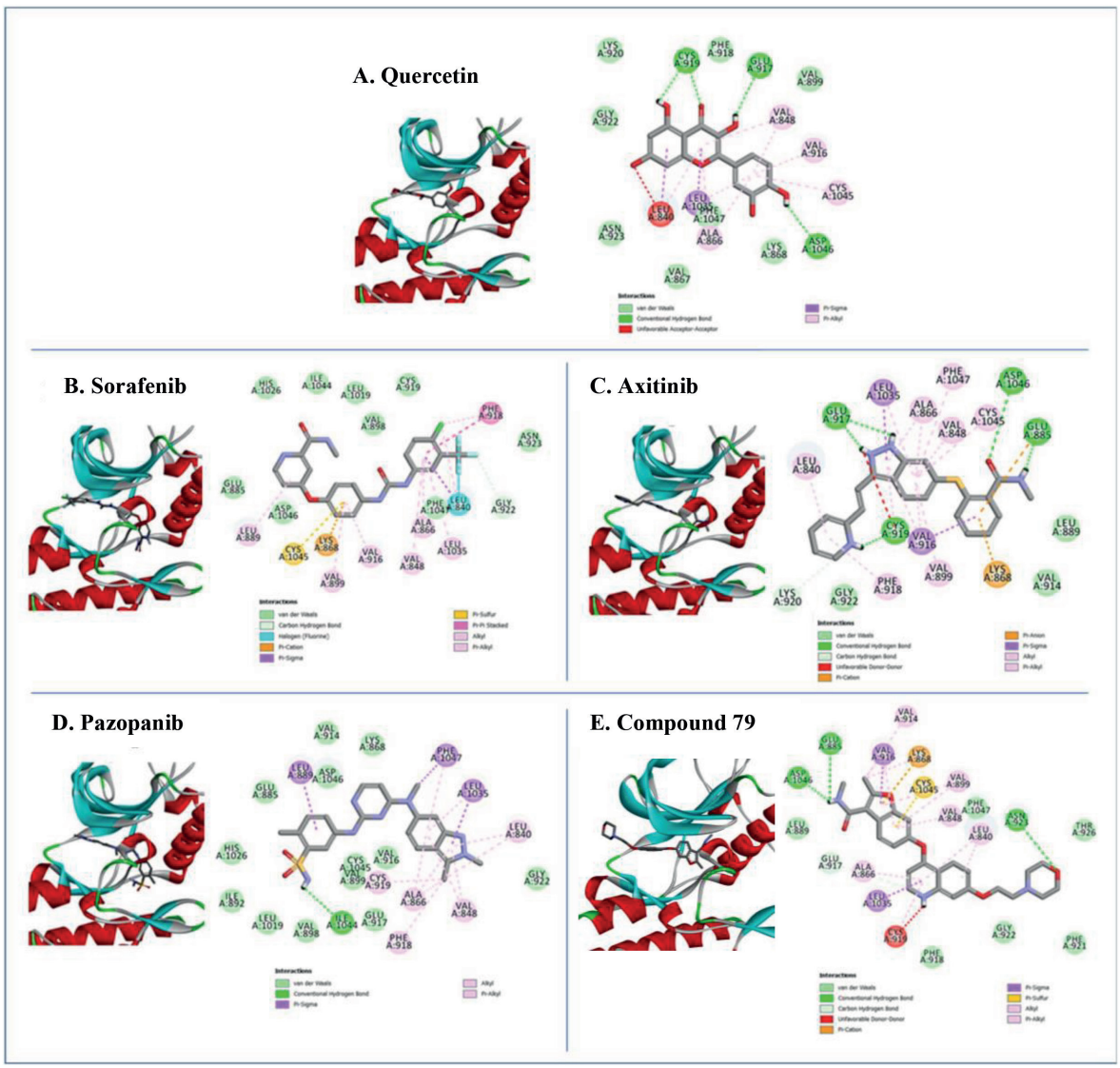

Figure 3 Docked conformations of (A) quercetin, (B) sorafenib, (C) axitinib, (D) pazopanib, and (E) compound 79 (PF-0033721) (PDB ID: 2XIR) to the VEGFR2 kinase domain, accompanied by their 2D interaction diagram.

Conclusion

This study highlights the medicinal potential of five phytochemical constituents namely, luteolin, quercetin, isorhamnetin, apigenin, and kaempferol, from *Houttuynia cordata* Thunb. as anti-angiogenic agents and VEGFR inhibitors with acceptable oral pharmacokinetics for the treatment of melanoma, which were identified using virtual screening. Specifically, apigenin and quercetin were predicted to be the strongest

VEGFR1 and VEGFR2 inhibitors, respectively. In this study, it is proposed that the compounds inhibit VEGFR through an unreported mechanism of action; direct inhibition of VEGFR at the ATP binding site. Apigenin and quercetin were proposed for further *in vitro* verification for VEGFR inhibition such as VEGFR protein-based inhibition assays, and further *in vivo* test such as evaluation of toxicity and oral pharmacokinetics in mice. Additionally, examining the synergistic effects of these phytochemicals with existing VEGFR inhibitors could provide a basis for developing combination therapies to enhance efficacies against melanoma.

References

1. D'Aguanno S, Mallone F, Marenco M, et al. Hypoxia-dependent drivers of melanoma progression. J. Exp. Clin. Cancer Res. 2021; 40 (1):159. doi: 10.1186/s13046-021-01926-6.
2. Meierjohann S. Hypoxia-independent drivers of melanoma angiogenesis. Front Oncol. 2015; 5: 102. doi.org/ 10.3389/fonc.2015.00102.
3. Mahabeleshwar GH, Byzova TV. Angiogenesis in melanoma. Semin Oncol. 2007; 34 (6): 555-65. doi: 10.1053/j.seminoncol.2007.09.009.
4. Jour G, Ivan D, Aung PP. Angiogenesis in melanoma: an update with a focus on current targeted therapies. J Clin Pathol. 2016; 69 (6): 472-83. doi: 10.1136/jclinpath-2015-203482.
5. Wu Z, Bian Y, Chu T, et al. The role of angiogenesis in melanoma: Clinical treatments and future expectations. Front Pharmacol. 2022; 13: doi.org/ 10.3389/fphar.2022.1028647.
6. Yang L, Jiang J-G. Bioactive components and functional properties of *Hottuynia cordata* and its applications. Pharm Biol. 2009; 47 (12): 1154-61. doi.org/10.3109/13880200 903019200.
7. Yang L, Chen G, Mohanty S, et al. GPR56 Regulates VEGF production and angiogenesis during melanoma progression. Cancer Res. 2011; 71 (16): 5558-68.
8. Hicklin DJ, Ellis LM. Role of the vascular endothelial growth factor pathway in tumor growth and angiogenesis. J Clin Oncol. 2005; 23 (5): 1011-27.
9. Yanarojana M, Nararatwanchai T, Thairat S, et al. Antiproliferative Activity and Induction of Apoptosis in Human Melanoma Cells by Houttuynia cordata Thunb Extract. Anticancer Res. 2017; 37 (12): 6619-28.
10. Kumar M, Prasad SK, Hemalatha S. A current update on the phytopharmacological aspects of *Houttuynia cordata* Thunb. Pharmacogn Rev. 2014; 8 (15): 22-35.
11. Sasidharan A, Surendran A, Rajagopal R, et al. Allspice (Pimenta dioica) essential oil mediates sphingosine kinase inhibition and subsequent induction of apoptosis in gastric cancer cells. Journal of Essent Oil-Bear Plants. 2024; 27 (2): 537-46.
12. Kim S, Chen J, Cheng T, et al. PubChem 2019 update: improved access to chemical data. Nucleic Acids Res. 2019; 47(D1): D1102-d9.
13. Kim S, Chen J, Cheng T, et al. PubChem in 2021: new data content and improved web interfaces. Nucleic Acids Res. 2021;49(D1): D1388-95.
14. O'Boyle NM, Banck M, James CA, et al. Open Babel: An open chemical toolbox. J Cheminform. 2011; 3 (1): 33.
15. Dallakyan S, Olson AJ. Small-molecule library screening by docking with PyRx. Methods Mol Biol. 2015; 1263: 243-50.

16. Berman HM, Westbrook J, Feng Z, et al. The Protein Data Bank. Nucleic Acids Res. 2000; 28 (1): 235-42.
17. Trott O, Olson AJ. AutoDock Vina: improving the speed and accuracy of docking with a new scoring function, efficient optimization and multithreading. J Comput Chem. 2010; 31 (2): 455-61.
18. Lipinski CA, Lombardo F, Dominy BW, et al. Experimental and computational approaches to estimate solubility and permeability in drug discovery and development settings. Adv Drug Deliv Rev. 1997; 23 (1): 3-25.
19. Liu LZ, Fang J, Zhou Q, et al. Apigenin inhibits expression of vascular endothelial growth factor and angiogenesis in human lung cancer cells: implication of chemoprevention of lung cancer. Mol Pharmacol. 2005; 68 (3): 635-43.
20. Fu J, Zeng W, Chen M, et al. Apigenin suppresses tumor angiogenesis and growth via inhibiting HIF-1α expression in non-small cell lung carcinoma. Chem -Biol Interact. 2022; 361 :109966.
21. Xiong W, Zheng B, Liu D, et al. Quercetin inhibits endothelial & hepatocellular carcinoma cell crosstalk via reducing extracellular vesicle-mediated VEGFR2 mRNA transfer. Mol Carcinogen. 2024; 63 (11): 2254-68.
22. Uttarawichien T, Kamnerdnond C, Inwisai T, et al. Quercetin Inhibits Colorectal Cancer Cells Induced-Angiogenesis in Both Colorectal Cancer Cell and Endothelial Cell through Downregulation of VEGF-A/VEGFR2. Sci Pharm. 2021; 89 (2): 23.
23. Li F, Bai Y, Zhao M, et al. Quercetin inhibits vascular endothelial growth factor-induced choroidal and retinal angiogenesis in vitro. Ophthalmic Res. 2015; 53 (3): 109-16.
24. Pratheeshkumar P, Budhraja A, Son Y-O, et al. Quercetin Inhibits Angiogenesis Mediated Human Prostate Tumor Growth by Targeting VEGFR- 2 Regulated AKT/mTOR/P70S6K Signaling Pathways. PLOS ONE. 2012; 7 (10): e47516.
25. Arabi N, Torabi MR, Fassihi A, et al. Identification of potential vascular endothelial growth factor receptor inhibitors via tree-based learning modeling and molecular docking simulation. J Chemom. 2024; 38 (7): e3545.
26. Mathi P, Das S, Nikhil K, et al. Isolation and Characterization of the Anticancer Compound Piceatannol from Sophora Interrupta Bedd. Int J Prev Med. 2015; 6:101.
27. Maji S, Sadhukhan S, Pattanayak AK, et al. Antiangiogenic Potential of Beneficial Sterols from Parotoid Gland Secretion of Indian Common Toads (Duttaphrynus melanostictus) in the Coastal Region of the Indian Subcontinent: An In Vivo to In Silico Approach. ACS Omega. 2025; 10 (10): 10480-92.
28. Lv Y, Wang Y, Zheng X, et al. Reveal the interaction mechanism of five old drugs targeting VEGFR2 through computational simulations. J Mol Graph Model. 2020; 96:107538.
29. Modi SJ, Kulkarni VM. Vascular Endothelial Growth Factor Receptor (VEGFR-2)/KDR Inhibitors: Medicinal Chemistry Perspective. Med Drug Discov. 2019; 2:100009.
30. Rampogu S, Baek A, Park C, et al. Discovery of Small Molecules that Target Vascular Endothelial Growth Factor Receptor-2 Signalling Pathway Employing Molecular Modelling Studies. Cells. 2019; 8 (3): 269. doi: 10.3390/cells8030269.

Supplementary Materials

Table S1 List of phytochemicals in Houttuynia cordata Thunb., and VEGFR inhibitors.

No.	Name	PubChem CID Chemical structure
1	Luteolin 3′,4′,5,7-Tetrahydroxyflavone	5280445 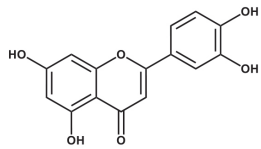
2	Quercetin 3,3′,4′,5,7-Pentahydroxyflavone	5280343 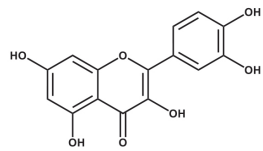
3	Isorhamnetin / 3-Methylquercetin / Quercetin 3’-methyl ether 3,5,7-trihydroxy-2-(4-hydroxy-3-methoxyphenyl)-4H-chromen-4-one	5281654 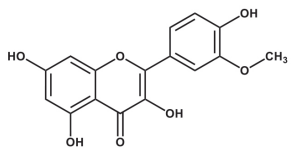
4	Quercitrin / Quercetin 3-rhamnoside 3′,4′,5,7-Tetrahydroxy-3-(α-L-rhamnopyranosyloxy) flavone	5280459 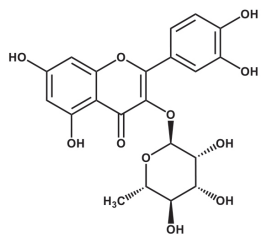
5	Isoquercitrin 3-(β-D-Glucopyranosyloxy)-3′,4′,5,7-tetrahydroxyflavone	5280804 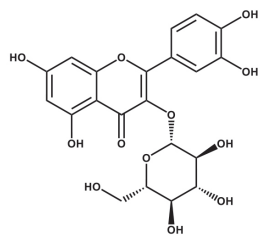
6	Hyperin / Hyperoside / Quercetin 3-galactoside 3-(β-D-Galactopyranosyloxy)-3′,4′,5,7-tetrahydroxyflavone	5281643 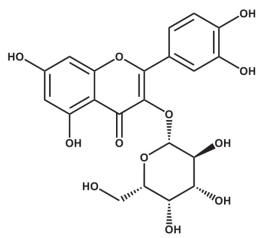

No.	Name	PubChem CID Chemical structure
7	Avicularin 3-(((2R,3S,4S,5R)-3,4-dihydroxy-5-(hydroxymethyl)tetrahydrofuran-2-yl)oxy)-2-(3,4-dihydroxyphenyl)-5,7-dihydroxy-4H-chromen-4-one	5490064 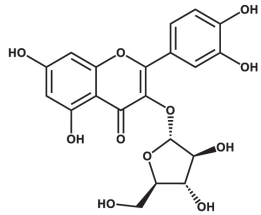
8	Rutin / Quercetin 3-rutinoside 3′,4′,5,7-Tetrahydroxy-3-[α-L-rhamnopyranosyl-(1→6)-β-D-glucopyranosyloxy]flavone	5280805 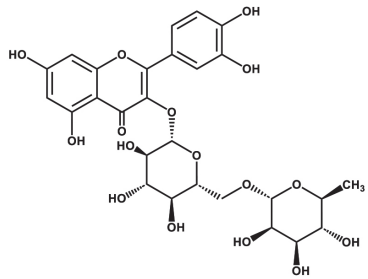
9	Catechin (2R,3S)-2-(3,4-dihydroxyphenyl)chromane-3,5,7-triol	9064 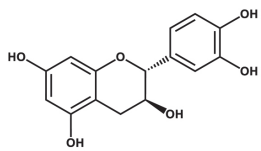
10	Apigenin 4′,5,7-Trihydroxyflavone	5280443 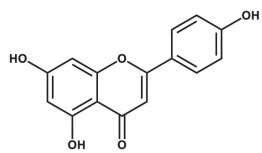
11	Kaempferol 3,5,7-trihydroxy-2-(4-hydroxyphenyl)-4H-chromen-4-one	5280863 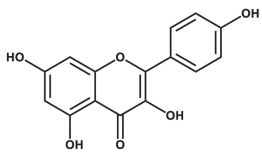
12	Afzelin / Kaempferol 3-rhamnoside 4′,5,7-Trihydroxy-3-(α-D-rhamnopyranosyloxy)flavone	5316673 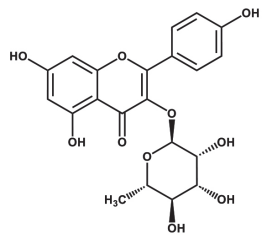
13	Phlorizin	6072 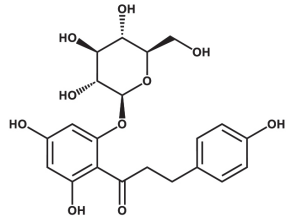

No.	Name	PubChem CID Chemical structure
14	Hesperidin (2S)-3′,5-Dihydroxy-4′-methoxy-7-[α-L-rhamnopyranosyl-(1→6)-β-D-glucopyranosyloxy]flavan-4-one	10621 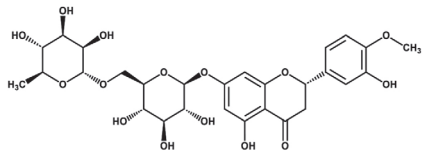
15	Genistin	5281377 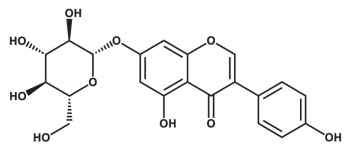
16	Aristolactam BII / Cepharanone B 1,2-dimethoxydibenzo[cd,f]indol-4(5H)-one	162739 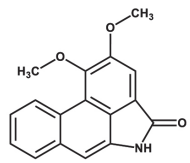
17	Aristolactam AII 2-hydroxy-1-methoxydibenzo[cd,f]indol-4(5H)-one	148657 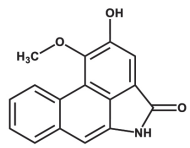
18	Piperolactam A / Aristolactam F1 1-hydroxy-2-methoxydibenzo[cd,f]indol-4(5H)-one	3081016 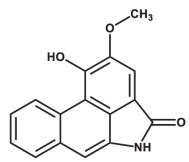
19	Caldensine 1,2-dimethoxy-5-methyldibenzo[cd,f]indol-4(5H)-one	21680139 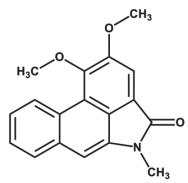
20	Splendidine 1,2,4-trimethoxy-7H-dibenzo[de,g]quinolin-7-one	196452 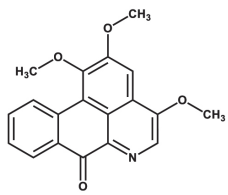
21	Lysicamine / Oxonuciferine 1,2-dimethoxy-7H-dibenzo[de,g]quinolin-7-one	122691 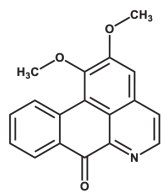

No.	Name	PubChem CID Chemical structure
22	Cepharadione B 1,2-dimethoxy-6-methyl-4H-dibenzo[de,g]quinoline-4,5(6H)-dione	189151 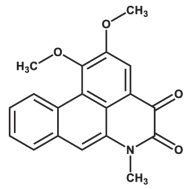
23	Norcepharadione B 1,2-dimethoxy-4H-dibenzo[de,g]quinoline-4,5(6H)-dione	189168 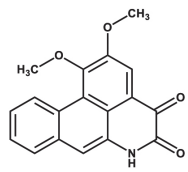
24	7-Chloro-6-demethylcepharadione B 7-chloro-1,2-dimethoxy-4H-dibenzo[de,g]quinoline-4,5(6H)-dione	131752718 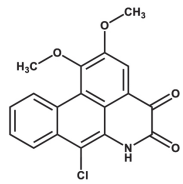
25	Noraristolodione 2-hydroxy-1-methoxy-4H-dibenzo[de,g]quinoline-4,5(6H)-dione	10108434 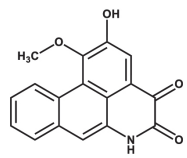
26	Chlorogenic Acid (1S,3R,4R,5R)-3-(((E)-3-(3,4-dihydroxyphenyl) acryloyl)oxy)-1,4,5-trihydroxycyclohexane-1-carboxylic acid	1794427 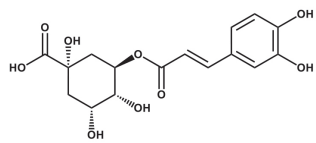
27	Neochlorogenic acid (1R,3R,4S,5R)-3-(((E)-3-(3,4-dihydroxyphenyl) acryloyl)oxy)-1,4,5-trihydroxycyclohexane-1-carboxylic acid	5280633 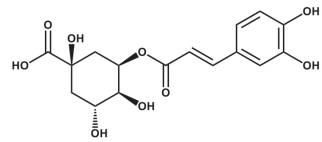
28	Cryptochlorogenic acid (3R,5R)-4-(((E)-3-(3,4-dihydroxyphenyl) acryloyl)oxy)-1,3,5-trihydroxycyclohexane-1-carboxylic acid	9798666 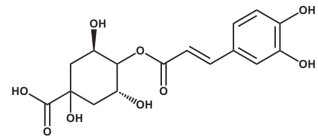
29	Procyanidin B1 (2R,2'R,3R,3'S,4R)-2,2'-bis(3,4-dihydroxyphenyl)-[4,8'-bichromane]-3,3',5,5',7,7'-hexaol	11250133 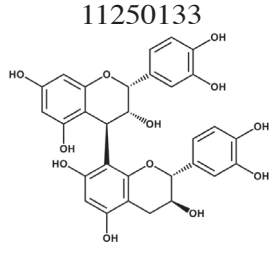

No.	Name	PubChem CID Chemical structure
30	β-Sitosterol / Stigmast-5-en-3β-ol	222284 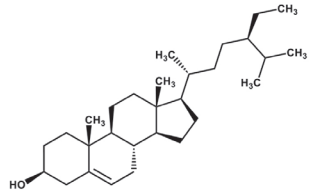
31	β-Sitosteryl glucoside	5742590 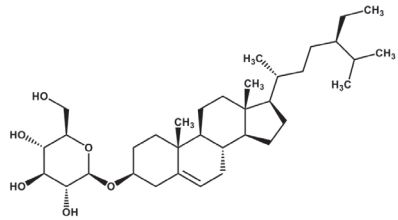
32	5-α-Stigmastane-3,6-dione	13992092 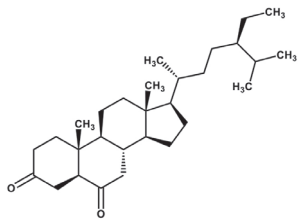
33	3-Hydroxy-β-sitost-5-en-7-one	160608 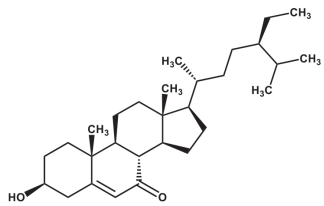
34	Cycloart-25-ene-3,24-diol	11419367 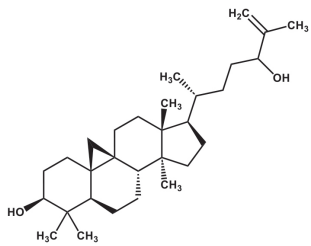
35	N-(1-hydroxy-3-phenylpropan-2-yl)benzamide	100005 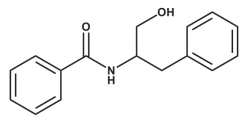
36	N-(4-hydroxyphenylethyl)benzamide	433864354 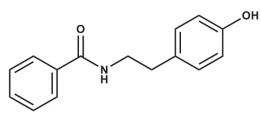
37	trans-N-(4-hydroxystyryl)benzamide	5369805 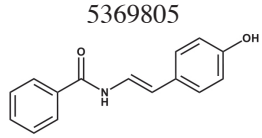

No.	Name	PubChem CID Chemical structure
38	Houttuynamide A	44521377 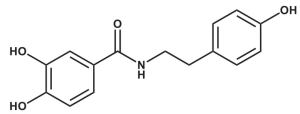
39	Houttuynoside A	44521323 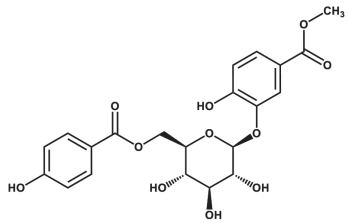
40	6,7-dimethyl-1-(2,4,5-trihydroxy-3-methylpentyl)-1,4-dihydroquinoxaline-2,3-dione	605462 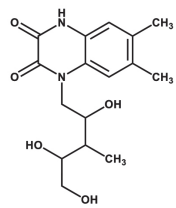
41	4-Hydroxyquinoline	69141 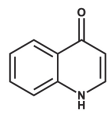
42	Benzamide / Phenylcarboxyamide	2331 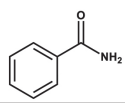
43	4-Hydroxybenzamide	65052 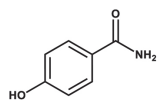
44	4-Hydroxy-3-methoxybenzamide	354088 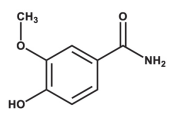
45	Vanillic acid	8468 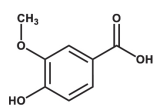
46	Methyl vanillate	19844 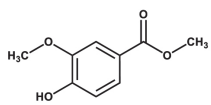
47	Vanillin	1183 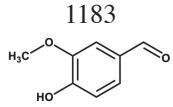

No.	Name	PubChem CID Chemical structure
48	Protocatehuic acid 3,4-dihydroxybenzoic acid	72 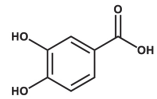
49	4-Hydroxybenzoic acid	135 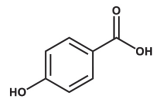
50	Methylparaben	7456 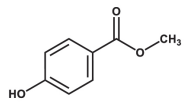
51	p-Hydroxybenzaldehyde	126 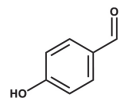
52	Methyl cis-ferulate	10176654 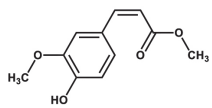
53	Methyl trans-ferulate	5357283 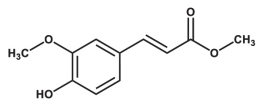
54	Benzyl-β-D-glucopyranoside	13254166 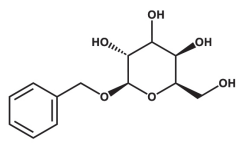
55	Methyl 3-hydroxybenzoate	88068 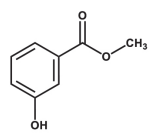
56	Methyl 4-(hydroxymethyl) benzoate	81325 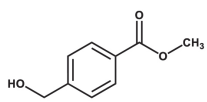
57	1,3,5-Tridecanoylbenzene	86173717 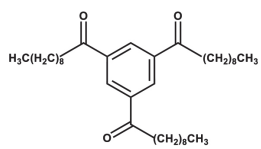
58	3,5-Didecanoylpyridine	85697557 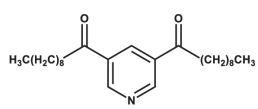

No.	Name	PubChem CID Chemical structure
59	5-Decanoyl-2-nonylpyridine	85697559 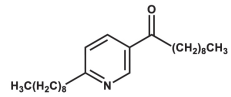
60	3,5-didecanoyl-4-nonyl-1,4-dihydropyridine	129711227 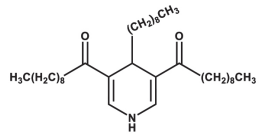
61	5-Methoxy-1-methylpyrrolidin-2-one	11423602 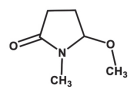
62	3-Nonyl-1H-pyrazole	24844218 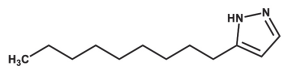
63	Myristicin	4276 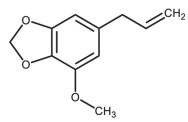
64	Elemicin	10248 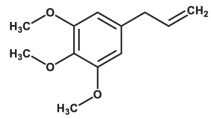
65	4-allyl-2,6-dimethoxyphenol	226486 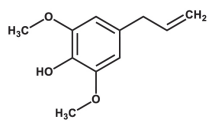
66	α-Asarone	636822 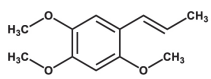
67	Indole-3-carboxylic acid	69867 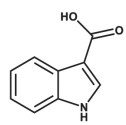
68	Vomifoliol	5280462 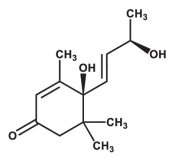
69	Dehydrovomifoliol	688492 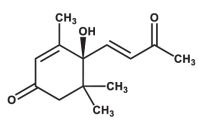

No.	Name	PubChem CID Chemical structure
70	Roseoside	73815023 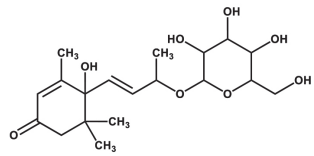
71	(E)-1-(3-hydroxybut-1-en-1-yl)-2,6,6-trimethylcyclohexane-1,2,4-triol	72751004 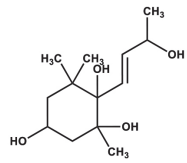
72	(E)-4-(1,2,4-trihydroxy-2,6,6-trimethylcyclohexyl) but-3-en-2-one	51136538 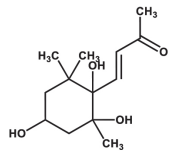
73	Quinic acid	6508 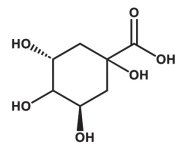
74	Caffeic Acid	689043 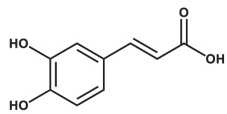
75	Sorafenib	216239 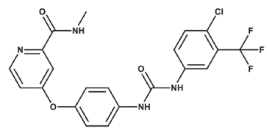
76	Axitinib	6450551 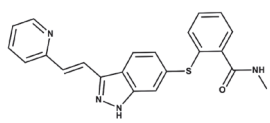
77	Pazopanib	10113978 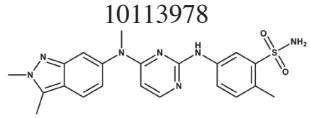
78	N-(4-Chlorophenyl)-2-((pyridin-4-ylmethyl)amino)benzamide (VEGFR tyrosine kinase inhibitor) (Native ligand in PBD ID: 3HNG)	9797919 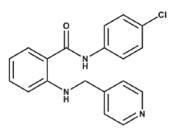
79	PF-00337210 (VEGFR2 tyrosine kinase inhibitor) (Native ligand in PBD ID: 2XIR)	11236560 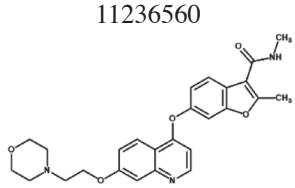

Table S2 The root mean square deviations of superimposed docked compounds to the VEGFRs. The compounds were docked at different exhaustiveness values.

Target	Compound	Exhaustiveness superimposition[b]	RMSD[d] (Å)
VEGFR1	Apigenin	10 & 15	0.019
		10 & 20	0.013
		15 & 20	0.013
	Quercetin	10 & 15	0.009
		10 & 20	0.005
		15 & 20	0.010
	Compound 78[a]	10 & 15	0.408
		10 & 20	0.353
		15 & 20	0.134
		Co-crystallized conformation[c] & 20	0.787
VEGFR2	Apigenin	10 & 15	6.884
		10 & 20	6.881
		15 & 20	0.013
	Quercetin	10 & 15	0.028
		10 & 20	0.014
	Compound 79[a]	15 & 20	0.029
		10 & 15	0.692
		10 & 20	2.089
		15 & 20	2.015
		Co-crystallized conformation[c] & 20	2.727

[a]Co-crystallized ligands; compounds 78 and 79 are N-(4-Chlorophenyl)-2-((pyridin-4-ylmethyl)amino)benzamide, and PF-00337210, respectively.
[b]Superimposition of docked conformations, in which the exhaustiveness values of 10, 15 and 20 were used.
[c]The conformations of the co-crystallized ligand was used.
[d]The DockRMSD web server was used to calculate the RMSDs (*J. Cheminform*. 2019, 11, 40).

Table S3 Binding energies (kcal/mol) of compounds docked with VEGFR1 and VEGFR2.

No.	Binding energy	
	VEGFR1	VEGFR2
1	-9.081	-9.907
2	-8.419	-9.945
3	-8.528	-9.839
4	-8.459	-8.671
5	-7.269	-7.536
6	-7.523	-7.550
7	-8.603	-8.119
8	-8.250	-8.397
9	-8.256	-8.906
10	-9.148	-9.879
11	-8.451	-9.936
12	-8.321	-7.654
13	-8.515	-9.137
14	-10.620	-10.051
15	-8.785	-9.375
16	-7.162	-8.116
17	-7.324	-8.122
18	-8.003	-8.073
19	-6.406	-7.697
20	-6.588	-8.003
21	-6.553	-8.087
22	-6.680	-8.437
23	-6.571	-8.221
24	-6.696	-8.655
25	-7.350	-8.275
26	-8.517	-8.004
27	-8.128	-8.506
28	-8.649	-8.918
29	-8.848	-7.950
30	-9.640	-8.876
31	-9.679	-8.219
32	-8.239	-8.847
33	-8.473	-7.429
34	-8.606	-8.019
35	-8.593	-8.665
36	-8.902	-8.723
37	-8.836	-9.060
38	-8.856	-8.776
39	-9.018	-8.980
40	-7.285	-7.570
41	-6.932	-6.689
42	-6.021	-5.741
43	-5.961	-6.007
44	-6.197	-6.226
45	-6.206	-6.072
46	-6.372	-6.434
47	-5.965	-5.937
48	-6.083	-6.217
49	-5.998	-5.863
50	-6.181	-6.238
51	-5.663	-5.708
52	-6.963	-6.758
53	-6.982	-7.340
54	-7.632	-7.627
55	-6.078	-6.180
56	-6.268	-6.320
57	-6.752	-7.681
58	-7.779	-7.713
59	-7.823	-7.858
60	-7.092	-6.947
61	-4.857	-4.669
62	-6.701	-6.711
63	-6.766	-6.659
64	-5.404	-5.626
65	-6.228	-5.814
66	-5.702	-6.568
67	-6.681	-6.705
68	-5.794	-6.010
69	-5.661	-5.998
70	-7.993	-7.171
71	-6.229	-6.65
72	-6.007	-6.254
73	-5.600	-5.821
74	-7.037	-7.600
75	-9.51	-8.946
76	-11.414	-10.065
77	-11.650	-10.492
78	-10.736	-9.477
79	-10.427	-11.168

Note: Compounds number according in Table S1